Hollow Stems for Higher Micromechanical Disk Resonator Quality Factor

Lingqi Wu, Mehmet Akgul, Zeying Ren, Yang Lin, Wei-Chang Li, and Clark T.-C. Nguyen
Department of Electrical Engineering and Computer Sciences
University of California at Berkeley, Berkeley, CA 94720 USA

Abstract—The use of hollow support stems to reduce energy loss to the substrate while supporting all-polysilicon UHF micromechanical disk resonators has enabled quality factors as high as 56,061 at 329 MHz and 93,231 at 178 MHz—values now in the same range as previous disk resonators employing multiple materials with more complex fabrication processes. With a substantially smaller cross-sectional area compared with the full stems used by predecessors, the hollow stem of this work effectively squeezes the energy conduit between the disk structure and the substrate, thereby suppressing energy loss and maximizing Q for devices operating in radial-contour and whispering gallery modes. Measurements confirm Q enhancements of 2.6× for contour modes at 154 MHz and 2.9× for wine glass modes around 112 MHz over values previously achieved by full stem all-polysilicon disk resonators with identical dimensions. The measured results not only demonstrate an effective Q-enhancement method with minimal increase in fabrication complexity, but also provide insights into anchor loss mechanisms that have been largely responsible for limiting the Q's attainable by all-polysilicon capacitively-transduced MEMS resonators.

Index Terms—anchor loss, hollow stem, micromechanical resonator, quality factor, communications, oscillator, filter.

I. Introduction

On chip capacitively transduced vibrating polysilicon micromechanical resonators have achieved Q's over 160,000 at 61 MHz [1] and larger than 14,000 at ~1.5 GHz [2], making them very attractive as on-chip frequency selecting and setting elements for filters and oscillators in wireless communication applications. The aforementioned Q's were achieved by first recognizing that anchor loss dominated at UHF, then using design strategies to suppress such loss, including attaching to the vibrating structure at nodal locations [3], minimizing support dimensions (e.g., reducing stem size [4]), using different materials for the support and vibrating structure to effect an energy reflecting impedance mismatch [5], and using quarter wavelength supports [3][6]. To date, oscillators employing the above high-Q resonators have already been demonstrated with phase noise performance commensurate with GSM cellular phone specifications for reference oscillators [1]. Still, there are applications, such as software-defined cognitive radio, that demand even higher Q's at RF to enable low-loss selection of single channels (rather than bands of them) to reduce the power consumption of succeeding electronic stages down to levels more appropriate for battery-powered handhelds.

Pursuant to further increasing Q at UHF, this work "hollows" the stems supporting all-polysilicon micromechanical disk resonators to effectively squeeze the energy conduit between
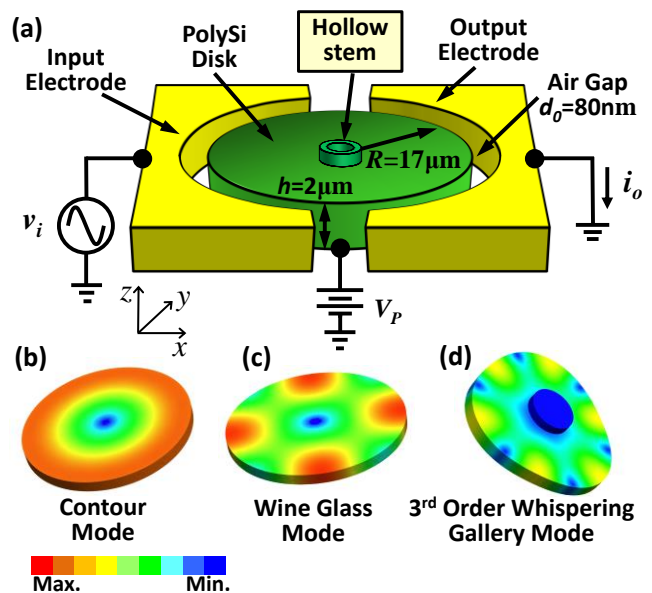

Fig. 1. *(a)* Schematic of an all-polysilicon hollow stem disk resonator in a two-port excitation and sensing configuration. *(b)* Contour mode shape. *(c)* Wine glass mode shape. *(d)* 3rd order whispering gallery mode (WGM) shape. (All simulated via FEM).

the disk structure and the substrate, thereby suppressing energy loss. Measurements confirm Q enhancements of 2.6× for contour modes at 154 MHz and 2.9× for wine glass modes around 112 MHz over values previously achieved by full stem all-polysilicon disk resonators with identical dimensions. Measured Q's as high as 56,061 at 329 MHz and 93,231 at 178 MHz further attest to the efficacy of this approach.

II. Hollow Stem Disk

Fig. 1(a) depicts the hollow stem disk resonator in a typical bias, excitation, and detection scheme. This device comprises a 2μm-thick disk surrounded by two closely spaced (d_o=80nm) electrodes and supported by an anchored stem attached at the center of the disk, where the radial displacement is minimized in each of the mode shapes shown in Fig. 1(b), (c), (d), making this attachment location a quasi-nodal point ("quasi", since the stem has finite radius). To minimize transducer loss that might otherwise mask the influence of anchor loss on Q, this device employs a capacitive transducer. The device is excited into resonance via a combination of a dc-bias voltage V_P applied to the conductive polysilicon resonant structure and an ac signal v_i applied to the input electrode, which together induce a force at the frequency of v_i that drives the disk into resonance vibration when the frequency of v_i matches the resonance frequency.
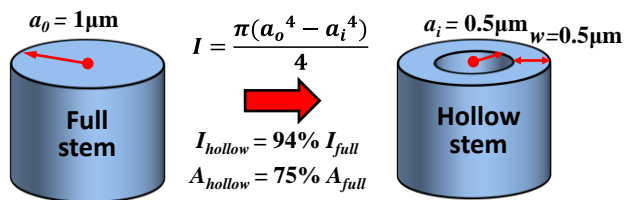
Fig. 2. Comparison of the strength (second moment of inertia I) and the cross sectional area A between a full stem with a_o=1μm and hollow stem with same a_o but a_i=0.5μm.

Once vibrating, the V_P-biased time varying capacitance between the disk and its output electrode generate an output current detectable by measurement instrumentation [4].

The main mechanism behind Q-enhancement via the hollow stem is essentially the same as that employed by [4]: reduction of the stem size to reduce its cross-sectional area and thereby reduce the conduit through which energy can pass from the vibrating disk structure to the substrate. In particular, by reducing stem sizes from 2.0μm to 1.6μm, [4] showed a measured Q increase from 5,551 to 14,657 for 405-MHz radial-contour mode disk resonators. In keeping with several theoretical studies in the literature [7] [8] [9], even higher Q's are expected as stem diameters decrease to submicron dimensions.

Unfortunately, there are of course practical barriers to continued scaling of stem diameters. First, as a stem is thinned, its support strength wanes, so there is a minimum stem diameter and length that can support a disk of a given size. Second, even if a stem maintained sufficient strength while scaled to nanometer dimensions, the need to not only form it, but also place it exactly at the disk center, poses fabrication challenges.

The hollow stem approach of Fig. 1 circumvents the above issues by employing a hollow cylinder with thin walls, rather than a single thin stem. Since the walls are thin, the cross-sectional area of the stem is still very small. However, as with all hollow cylinders (e.g., pipes, lances, etc.), it still retains much of the strength of a full stem with the same diameter, as summarized by the analysis of Fig. 2.

III. FABRICATION PROCESS

The fabrication process for the hollow stem devices in this work leverages heavily the self-aligned stem process of [4] that not only eliminates disk-to-stem misalignment, but also allows for different stem and disk film thicknesses, thereby greatly facilitating manufacture of hollow stems. The process begins with layer depositions and patternings (where appropriate) for the substrate ground plane and contacts (not shown), polysilicon interconnects, bottom sacrificial layer, and structural polysilicon capped by an oxide etch hard mask, all identical to those used in [4]. Like [4], instead of using an anchor mask to first define the stem then another mask aligned to the first to define the disk structure, this process defines both the stem hole position and the disk edges all in one mask, effectively eliminating the possibility of stem misalignment. This maximizes the Q of the ensuing device, since it allows centering of the stem precisely at the disk nodal location. After the single-mask lithography defining the disk and stem hole, the doped polysilicon structural layer is patterned through the oxide hard
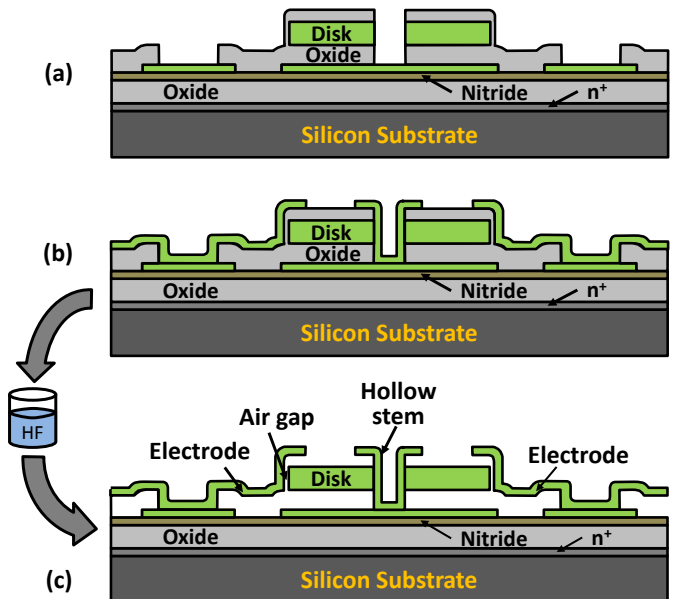

Fig. 3. Cross-sections showing the last few steps in the fabrication process for hollow stem, small-lateral-gap, all-polysilicon disk resonators.
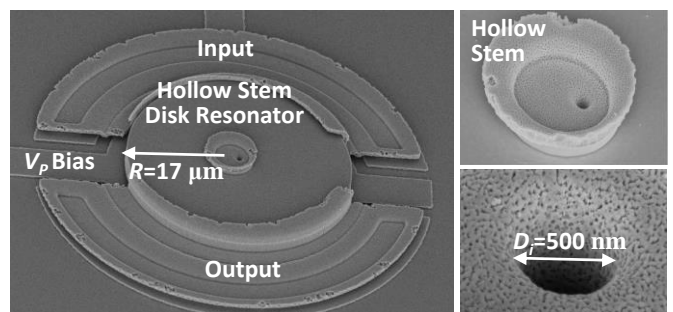

Fig. 4. SEM's of a fabricated polysilicon hollow stem disk resonator with zoom-in's to its hollow stem structure. The halo around the hollow stem results from over etch of the oxide hard mask when etching the stem via.

mask, then a sacrificial sidewall spacer oxide (to define the gap) is deposited via LPCVD to yield the cross-section of Fig. 3(a).

At this point, the process flow deviates from that of [4]. In particular, instead of depositing a 2μm thick polysilicon to fully refill the 1μm~3μm diameter stem holes, as was done previously, a very thin layer (less than 500nm) insufficient to refill the stem holes is deposited via LPCVD at 585°C followed by POCl$_3$ doping. The conformity of LPCVD polysilicon allows the film to follow the contours of the stem hole, even at corners.

Wafers are then immersed in 49 wt. % hydrofluoric acid for ~30 min. to etch away sacrificial oxide and release the structures, leaving the final cross-section of Fig. 3(c). Fig. 4 presents the SEM of a fabricated device with zoom-in's on its stem, which features 500nm-thick walls in a 1μm-outer radius stem hole, resulting in a 500nm-radius hollow region.

In addition to the thin-walled stem, the SEM of Fig. 4 also shows electrodes with equally thin walls. Like the stems, the electrodes also benefit from the increased strength of a curved geometry. , However, as will be seen in the next section, this increased geometrical strength might not always be sufficient.

IV. EXPERIMENTAL RESULTS
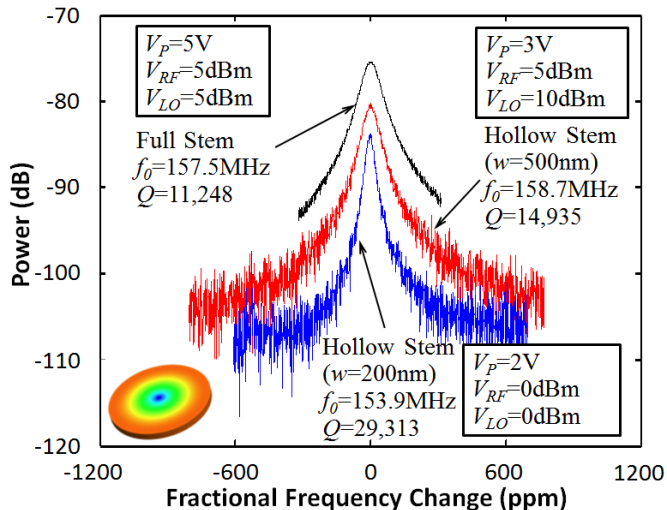
To gauge the Q-enhancing efficacy of hollow stems, meas-

Fig. 5. Comparison of frequency characteristics for full stem and hollow stem all-polysilicon disk resonators vibrating in the radial-contour mode.

urements on fabricated devices focus on comparison of conventional disk resonators with 2µm-diameter full stems with hollow stem resonators employing the same outer stem diameter, but different stem wall thicknesses of 200nm and 500nm. The devices were tested using the mixing measurement method described in [10] (that allows more accurate measurement of mechanical Q) under a 2µTorr vacuum environment generated by a Lakeshore FWPX cryogenic probe station. Although high frequency micromechanical resonators are less susceptible to gas damping, so are able to reach Q's on the order of 10,000 in air [5], vacuum is still needed to measure Q's above this.

To gauge the degree to which hollow stem design really suppresses energy loss to the substrate, the measurements also compare their efficacies for disks vibrating in each of the mode shapes depicted in Fig. 1(b)-(d). In particular, the FEM simulations shown actually depict displacements, where the darker the blue color, the less the displacement. A focus on the anchors reveals that whispering gallery modes, including the wine-glass mode, should allow much higher Q's than radial-contour modes if anchor losses dominate. In addition, hollow stem design should be less necessary for higher whispering gallery modes if high Q's are desired.

A. Radial-Contour Mode

Fig. 5 combines the measured frequency characteristics of a full stem radial-contour mode disk resonator together with ones sporting 500nm-wall and 200nm-wall hollow stems, all with identical 17-µm radii. To facilitate interpretation of the data, Fig. 5 plots measured output power along the *y*-axis against fractional frequency change relative to the resonance frequency of each device along the *x*-axis. Here, the 200nm-wall hollow stem device achieves a Q of 29,313 at 153.9 MHz, which is more than 2.6× higher than its identically-dimensioned full stem counterpart. The 500nm-wall hollow stem device also provides an improvement, although smaller, at about 1.3× better than the full stem case. The smaller the hollow stem wall thickness, the larger the improvement in Q, all confirming the discussion of Section II.

As indicated by the RF and LO voltage values used in mixing

measurements for Fig. 5, the 200nm-wall hollow stem device could not accept voltages as large as used for the 500nm-wall hollow stem and full stem devices, since the former tended to pull into its electrodes when voltages exceeded 3V. This explains the lower peak current measured for this device despite its much higher Q. It also reveals a limitation of the hollow stem approach, where the much thinner stem, combined with much thinner electrodes, compromises the maximum dc-bias voltage sustainable across the electrode-to-resonator gap before pull-in. As mentioned in Section III, although the cylindrical and curved geometries of the stem and electrodes, respectively, do help to strengthen them, they seem not as strong as full stem or thicker counterparts.

B. Wine-Glass Mode

Although the input and output electrodes of the device under test are designed for radial-contour mode vibration, they are also able to excite and detect the wine glass mode depicted in Fig. 1(c), since both modes have large vibration amplitudes centered over the output electrodes. Fig. 6 presents a plot similar to that of Fig. 5, but this time comparing wine glass modes for the different devices. The highest Q is now 45,138 at 112 MHz, again for the 200nm-wall hollow stem disk. As with the radial mode, the Q's of the wine-glass mode also improve with decreasing hollow stem thickness, with a 2.9× improvement for the 200nm-wall hollow stem versus full stem.

C. Whispering Gallery Modes

The wine-glass mode is actually just one of the many whispering gallery modes [11] of the disk structure shown in Fig. 1(c)-(d). In the wine-glass mode, there are two positive vibration amplitude maxima, making it a 2nd order whispering gallery mode (WGM). The mode in Fig. 1(d) is a 3rd order WGM with 3 maxima. Whispering gallery modes differ from the radial-contour mode in that their acoustic wave propagates around the disk periphery, rather than the radial direction. Thus, while the radial-contour mode undergoes tremendous volume expansion and contraction during vibration, a whispering gallery mode conserves its volume, resulting in less displacement near the center of the disk, hence less Poisson expansion along the z-axis at the stem location. This then leads to smaller energy loss to the substrate and higher Q, which is consistent with the measurement results showing that wine glass mode Q for the 200nm-wall hollow stem disk in Fig. 6 is larger than the highest posted by the radial-contour mode devices of Fig. 5.

Higher order WGM's, such as the 3rd order one of Fig. 1(d), further exhibit a dramatically larger displacement-free area around their stems than lower order ones, as shown in the displacement FEM simulations of Fig. 1(c) and (d). This indicates that the former should lose less energy through the stem to the substrate no matter the type of stem, suggesting that higher order whispering gallery modes should post even higher Q's that are less dependent upon stem design, i.e., the Q should be high whether or not a hollow stem is used.

To confirm the above, Fig. 7 presents a plot similar to that of Fig. 5 and Fig. 6, but this time comparing 3rd order WGM's for the different devices. The highest measured Q is now 93,231 at

L. Wu, M. Akgul, Z. Ren, Y. Lin, W.-C. Li, T. Rocheleau, and C. T.-C. Nguyen, "Hollow stems for higher UHF microme-chanical disk resonator quality factor," *Proceedings*, 2010 IEEE Int. Ultrasonics Symp., Orlando, FL, Oct. 18-21, 2011.
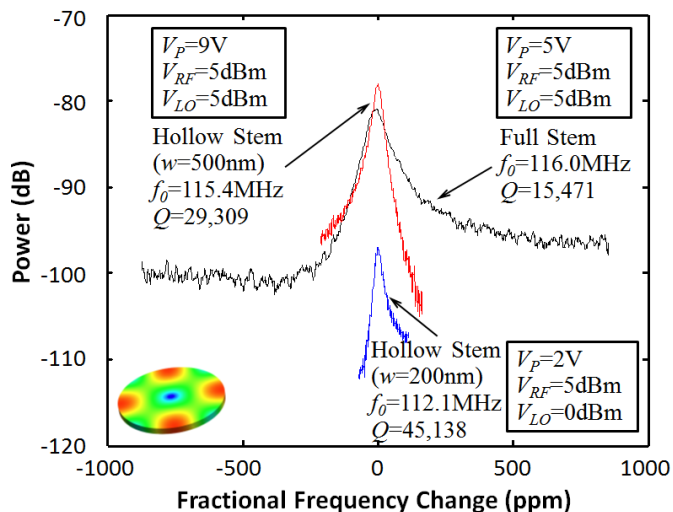
Fig. 6. Comparison of frequency characteristics of full stem and hollow stem all-polysilicon disk resonators vibrating in the wine glass mode.
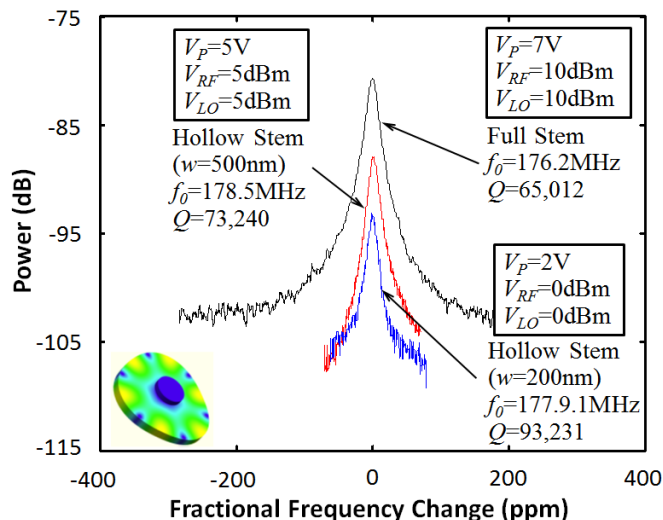

Fig. 7. Comparison of frequency characteristics for full stem and hollow stem all-polysilicon disks vibrating in the 3rd-order whispering gallery mode.

Fig. 8. Measured frequency characteristic for a hollow stem polysilicon disk resonator vibrating in its 6th order whispering gallery mode.

177.9 MHz, again for the 200nm-wall hollow stem disk. As predicted, this is much higher than exhibited by the other modes depicted in Fig. 5 and Fig. 6. Although impressive, the Q of this device is only 1.4× higher than that of the same mode of the full stem device, which posts a Q of 65,012 at 176.2 MHz that is still quite large. Thus, hollow stem design is still beneficial for whispering gallery modes, but its benefits over a full stem diminish as mode order increases.

As a final UHF demonstration, Fig. 8 plots the frequency characteristics of a 17μm-radius disk employing a 500nm-thick hollow stem to achieve a Q of 56,061 at 329 MHz while vi-brating in its 6th order whispering gallery mode.

V. CONCLUSIONS

The measured Q enhancements in this work of 2.6× for hollow stem radial-contour mode disk resonators at 154 MHz and 2.9× for wine glass mode ones at 112 MHz versus identi-cally dimensioned full stem counterparts confirms the efficacy of the hollow stem approach for maximizing resonator Q. This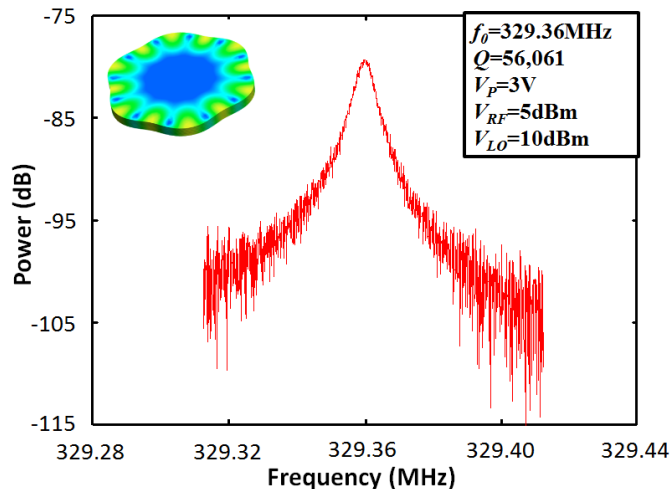 approach not only circumvents lithography challenges other-wise needed by other stem-size reducing Q-enhancement ap-proaches, but does so with zero increase in fabrication com-plexity over conventional methods for achieving stemmed resonators, making it a very simple and effective way to en-hance quality factor. In the lower UHF range (around 329 MHz), a Q of 56,061 is achieved by a hollow stem disk reso-nator vibrating in its 6th order whispering gallery mode, which is high enough to build RF front-end channel-select filters and low phase noise local oscillators for the low end of next gen-eration wireless architectures, such as software-defined cogni-tive radios. Similar Q's are needed at even higher frequencies, where the hollow stem approach should be even more effective.

REFERENCES

[1] Y.-W. Lin, S.-S. Li, Z. Ren, and C. T.-C. Nguyen, "Low phase noise array-composite micromechanical wine-glass disk oscillator," *Technical Digest, IEEE Int. Electron Devices Mtg.*, 2005, pp. 287-290.

[2] S.-S. Li, Y.-W. Lin, Y. Xie Z. Ren, and C. T.-C. Nguyen, "Microme-chanical hollow-disk ring resonators," *Proceedings, MEMS'04*, Maas-tricht, The Netherland, pp. 821-824.

[3] K. Wang, A.-C. Wong, and C. T.-C. Nguyen, "VHF free-free beam high-Q micromechanical resonators," *J. Microelectromech. Syst.*, vol. 9, no. 3, pp. 347-360, Sept.2000.

[4] J. Wang, Z. Ren, and C. T.-C. Nguyen, "1.156-GHz self-aligned vibrating micromechanical disk resonator," *IEEE T. Ultrason. Ferr.*, vol. 51, no. 12, pp. 1607-1628, Dec. 2004.

[5] J. Wang, J. E. Butler, T. Feygelson, and C. T.-C. Nguyen, "1.51-GHz polydiamond micromechanical disk resonator with impedance mis-matched isolating support," *Proceedings, MEMS'04*, Maastricht, The Netherlands, pp. 641-644.

[6] R. Jansen, *et al.*, "Optimal T-support anchoring for bar-type BAW reso-nators," *Proceedings, MEMS'11*, Cancun, Mexico, pp. 609-612.

[7] Z. Hao, and Y. Xu, "Vibration displacement on substrate due to time-harmonic stress sources from a micromechanical resonator," *Jour-nal of Sound and Vibration*, vol. 322, no. 1-2, pp. 196-215, Apr. 2009.

[8] D. S. Bindel1 and S. Govindjee, "Elastic PMLs for resonator anchor loss simulation," *Int'l Journal for Numerical Methods in Engineering*, vol. 64, no. 6, pp. 789-818, Oct. 2005.

[9] Y.-H. Park and K. C. Park, "High-Fidelity Modeling of MEMS Resona-tors—Part I: Anchor Loss Mechanisms Through Substrate," *J. Microe-lectromech. Syst.*, vol. 12, no. 3, Apr. 2004.

[10] A.-C. Wong and C. T.-C. Nguyen, "Micromechanical mixer-filters", *J. Microelectromech. Syst.*, vol. 13, no. 1, pp. 100-112, Feb. 2004.

[11] J. W. Strutt (Lord Rayleigh), *The Theory of Sound*. Dover: New York, 1945.